Supplemental Materials

Molecular Biology of the Cell

Varlakhanova et al.

Table S1: Plasmids used in this work:

Plasmid	Details	Source
S cer.PAR32	pRS316 *S cer.PAR32*	This work
S cer.PAR32 4x mut	pRS315 *S cer.PAR32* 4x GRGGAG-AAAAAA	This work
S cer. PAR32 N295A	pRS316 *S cer. PAR32* N295A	This work
S cer. PAR32 K291A	pRS316 *S cer. PAR32* K291A	This work
*S cer. PAR32*Δ288-295	pRS316 *S cer. PAR32*Δ288-295	This work
*S cer. PAR32*Δ276-295	pRS316 *S cer. PAR32*Δ276-295	This work
S cer.PAR32-EGFP	pRS316 *S cer.PAR32*-EGFP	This work
S cer.PAR32 4x mut-EGFP	pRS315 *S cer.PAR32* 4x GRGGAG-AAAAAA-EGFP	This work
S cer. PAR32 N295A-EGFP	pRS316 *S cer. PAR32* N295A-EGFP	This work
S cer. PAR32 K291A-EGFP	pRS316 *S cer. PAR32* K291A-EGFP	This work
*S cer. PAR32*Δ276-295-EGFP	pRS316 *S cer. PAR32*Δ276-295-EGFP	This work
*S cer. PAR32*Δ288-295-EGFP	pRS316 *S cer. PAR32*Δ288-	This work

	295-EGFP	
S cer.PAR32-3xHA	pRS316 *S cer. PAR32*-3xHA	(Varlakhanova et al., 2017)
S cer.PAR32 4xmut-3xHA	pRS316 *S cer. PAR32* 4xmut-3xHA	This work
S cer.PAR32 N295A-3xHA	pRS316 *S cer. PAR32* N295A-3xHA	This work
S cer.PAR32 K291A-3xHA	pRS316 *S cer. PAR32* K291A-3xHA	This work
*S cer.PAR32*Δ276-295-3xHA	pRS316 *S cer. PAR32*Δ276-295-3xHA	This work
*S cer.PAR32*Δ288-295-3xHA	pRS316 *S cer. PAR32*Δ288-295-3xHA	This work
NLS-*PAR32*	pRS316 NLS-*S cer. PAR32*	This work
NLS-*PAR32* 4x mut	pRS316 NLS-*S cer. PAR32* 4x GRGGAG-AAAAAA	This work
NLS-*PAR32*-EGFP	pRS316 NLS-*S cer. PAR32*-EGFP	This work
NLS-*PAR32* 4x mut-EGFP	pRS316 NLS-*S cer. PAR32* 4x GRGGAG-AAAAAA-EGFP	This work
GAP1-lacZ	pRS314 *GAP1*prom-*GAP1* 1-53-*E. coli* lacZ 10-end	This work

TOR1 L2134M	pRS426 *S cer*. *TOR1* L2134M	(Varlakhanova et al., 2017)
EGFP-*TOR1*	pRS316 EGFP-*S cer. TOR1*	(Varlakhanova et al., 2017)
NLS-BFP	pRS314 *TEF1* prom-NLS-TagBFP	This work
GAP1-GFP	pRS416 *GAP1*prom-*GAP1*-GFP	Allyson O'Donnell

Table S2: Strains used in this work

W303A	*MAT***a**; *ade2-1*; *leu2-3,112*; *his3-11,15*; *trp1-1*; *ura3-1*; *can1-100*	
PY_126	*MAT***a**; *ade2-1*; *leu2-3,112*; *his3-11,15*; *trp1-1*; *ura3-1*; *can1-100*; Δ*pib2*::KAN	(Varlakhanova et al., 2017)
PY_150	*MAT***a**; *ade2-1*; *leu2-3,112*; *his3-11,15*; *trp1-1*; *ura3-1*; *can1-100*; Δ*npr1*::NAT	(Varlakhanova et al., 2017)
PY_154	*MAT***a**; *ade2-1*; *leu2-3,112*; *his3-11,15*; *trp1-1*; *ura3-1*; *can1-100*; Δ*par32*::NAT	This work
PY_164	*MAT***a**; *ade2-1*; *leu2-3,112*; *his3-11,15*; *trp1-1*; *ura3-1*; *can1-100*; Δ*npr1*::KAN Δ*par32*::NAT	This work
PY_178	*MAT***a**; *ade2-1*; *leu2-3,112*; *his3-11,15*; *trp1-1*; *ura3-1*; *can1-100*; Δ*mep1*::KAN; Δ*mep3*::*HIS3*	This work
PY_180	*MAT***a**; *ade2-1*; *leu2-3,112*; *his3-11,15*; *trp1-1*; *ura3-1*; *can1-100*; Δ*mep1*::KAN; Δ*mep3*::*HIS3*; Δ*npr1*::NAT	This work
PY_184	*MAT***a**; *ade2-1*; *leu2-3,112*; *his3-11,15*; *trp1-1*; *ura3-1*; *can1-100*; Δ*mep1*::KAN; Δ*mep3*::*HIS3*; Δ*par32*::NAT	This work
PY_194	*MAT***a**; *ade2-1*; *leu2-3,112*; *his3-11,15*; *trp1-1*; *ura3-1*; *can1-100*; Δ*gat1*::*HIS3*	This work
PY_198	*MAT***a**; *ade2-1*; *leu2-3,112*; *his3-11,15*; *trp1-1*;	This work

	ura3-1; *can1-100*; ∆*par32*::*NAT*; ∆*gat1*::*HIS3*	
PY_208	*MAT***a**; *ade2-1*; *leu2-3,112*; *his3-11,15*; *trp1-1*; *ura3-1*; *can1-100*; ∆*gln3*::*HIS3*	This work
PY_210	*MAT***a**; *ade2-1*; *leu2-3,112*; *his3-11,15*; *trp1-1*; *ura3-1*; *can1-100*; ∆*par32*::*NAT*; ∆*gln3*::*HIS3*	This work

Figure S1. (A) Expression of a constitutively active Tor1 mutant allele partially rescues the Δ*par32* rapamycin sensitivity. Exponentially-growing W303A or Δ*par32*cells (OD_{600} 0.6-0.8) expressing the *TOR1* L2134M as indicated were treated with rapamycin (200 ng/ml in YPD) for 5 hr at 30 °C. Cells were then washed and plated on YPD. Cells were imaged after incubation for 2 days at 30 °C. (B) Quantifications of differences in plasma membrane to cytosol (left charts) and nucleus to cytosol (right charts) ratios of Par32-EGFP expressed in W303A (upper charts) or Δ*npr1*(lower charts) cells. Growth conditions and treatment times as indicated. Differences in means of membrane to cytosol ratios in W303A and Δ*npr1* cells were significantly heterogeneous (one-way ANOVA: W303A – $F_{4,31}$ = 4.29 hence p = 0.007; Δ*npr1* – $F_{4,31}$ = 10.33 hence p = 1.95E-5). Similarly, differences in means of nucleus to cytosol ratios in W303A and Δ*npr1* cells were significantly heterogeneous (one-way ANOVA: W303A – $F_{4,35}$ = 34.19 hence p = 1.21E-11; Δ*npr1* – $F_{4,36}$ = 13.07 hence p = 1.14E-6). Significantly different pairs of means, as assessed by the post-hoc Tukey HSD test, are indicated (*, p< 0.05; **, p< 0.01).

Figure S2. Par32 subcellular localization in cells grown in different carbon sources. W303A cells expressing Par32-EGFP were grown in glucose (YPD), ethanol / glycerol (YPEG) or galactose (YPGAL). The plasma membrane stained with 10 μM FM 4-64 for 30 min on ice prior to visualization. Scale bar 5 μm.

Figure S3. Nuclear localization of Par32 depends on the four conserved GRGGAGNI motifs. W303A and Δ*npr1* cells expressing the indicated EGFP-tagged Par32 construct as well as NLS-BFP (NLS – SV40 Large T Antigen nuclear localization sequence) were grown under conditions of nitrogen starvation (SD –N) for 3 hr prior to imaging. The plasma membrane stained with 10 μM FM 4-64 for 30 min on ice prior to visualization. Scale bar 5 μm.

Figure S4. (A) Nuclear localization of NLS-Par32 and NLS-Par32 4x mut in W303A and Δ*par32* cells. W303A or Δ*par32* cells expressing the indicated EGFP-tagged NLS-Par32 fusion (SV40 Large T Antigen nuclear localization sequence) were grown in SC. (B) Rapamycin treatment does not prevent nuclear accumulation of EGFP-tagged NLS-Par32. W303A or Δ*par32* cells expressing NLS-Par32-EGFP were treated with rapamycin (200 ng/ml, 3 hr) prior to imaging. (C) Plasma membrane association of Par32 is Mep1- and Mep3-independent. Δ*mep1* Δ*mep3* Δ*npr1* cells expressing Par32-EGFP were grown in SC or SD-N for 3 hr prior to imaging. The plasma membrane was labeled with 10 μM FM 4-64 for 30 min on ice prior to visualization.Scale bars 5 μm.

Figure S5. Deletion of Gat1 (A) or Gln3 (B) does not rescue the defect in recovery from rapamycin exposure of Δ*par32* cells. Exponentially-growing (OD_{600} 0.6-0.8)cells, as indicated, were untreated or treated with rapamycin (200 ng/ml in YPD) for 5 hr at 30 °C. Cells were then washed and plated on YPD. Cells were imaged after incubation for 2 days at 30 °C. The left-

most spot in each case corresponds to 2 μl of a culture with OD_{600} 0.5. Spots to the right of this correspond to 2 μl of sequential 5-fold dilutions.

A

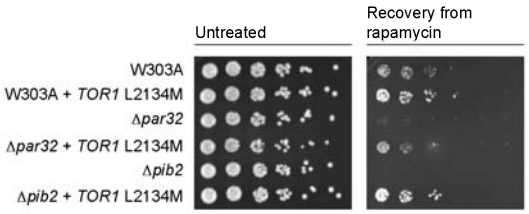
Untreated
Recovery from rapamycin
W303A
W303A + TOR1 L2134M
Δpar32
Δpar32 + TOR1 L2134M
Δpib2
Δpib2 + TOR1 L2134M

B

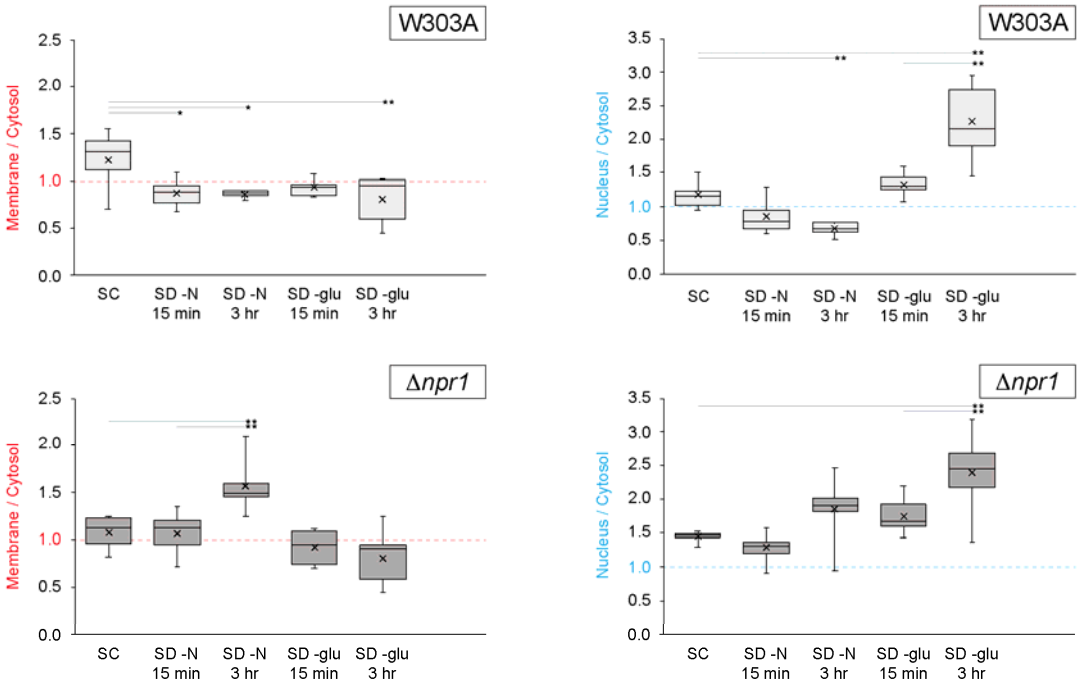
W303A
Membrane / Cytosol
Nucleus / Cytosol
Δnpr1
SC
SD -N 15 min
SD -N 3 hr
SD -glu 15 min
SD -glu 3 hr

Fig. S1

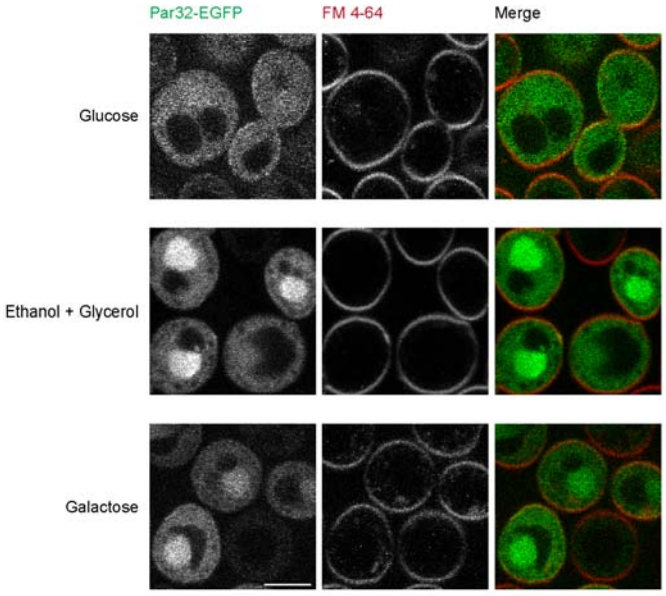
Par32-EGFP
FM 4-64
Merge
Glucose
Ethanol + Glycerol
Galactose

Fig. S2

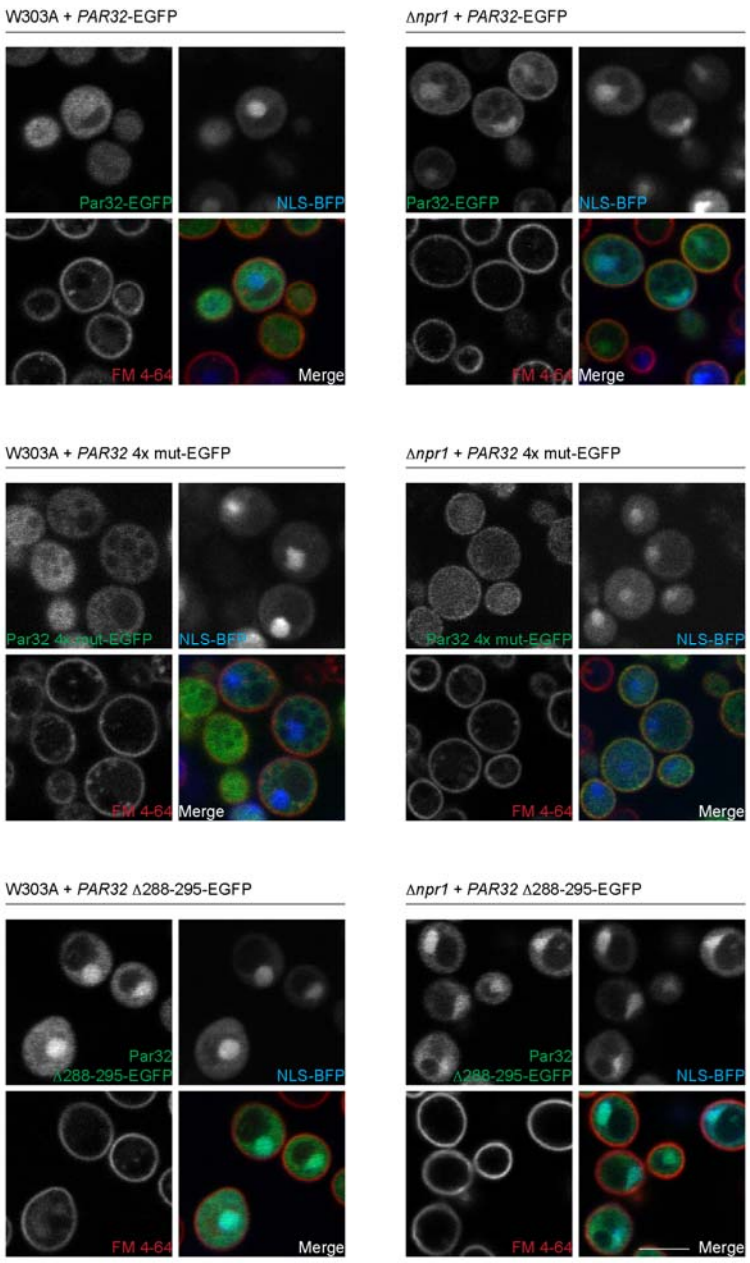
W303A + PAR32-EGFP
Par32-EGFP
NLS-BFP
FM 4-64
Merge
Δnpr1 + PAR32-EGFP
Par32-EGFP
NLS-BFP
FM 4-64
Merge
W303A + PAR32 4x mut-EGFP
Par32 4x mut-EGFP
NLS-BFP
FM 4-64
Merge
Δnpr1 + PAR32 4x mut-EGFP
Par32 4x mut-EGFP
NLS-BFP
FM 4-64
Merge
W303A + PAR32 Δ288-295-EGFP
Par32 Δ288-295-EGFP
NLS-BFP
FM 4-64
Merge
Δnpr1 + PAR32 Δ288-295-EGFP
Par32 Δ288-295-EGFP
NLS-BFP
FM 4-64
Merge

Fig. S3

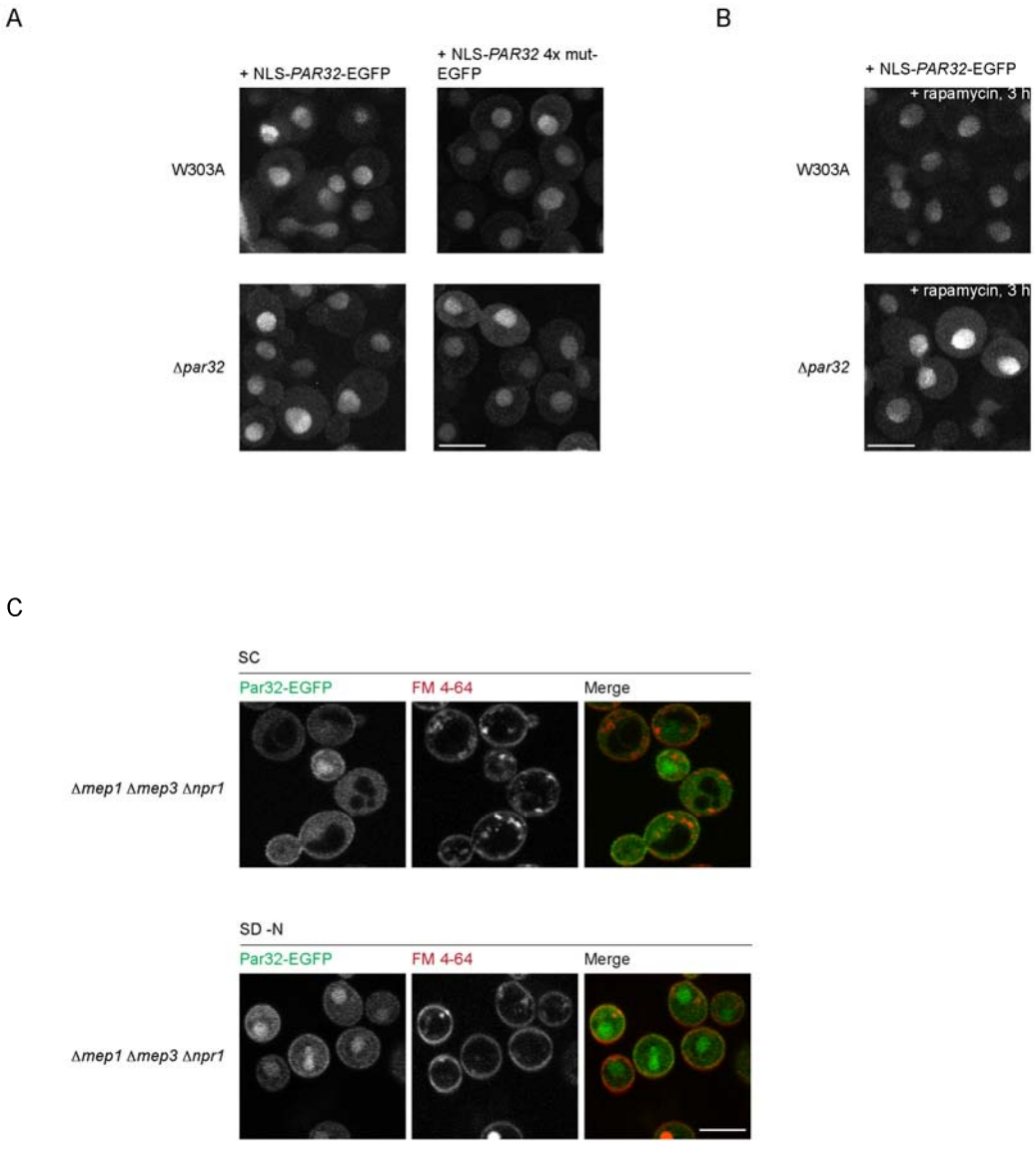
A
+ NLS-PAR32-EGFP
+ NLS-PAR32 4x mut-EGFP
W303A
Δpar32
B
+ NLS-PAR32-EGFP
+ rapamycin, 3 h
W303A
Δpar32
C
SC
Par32-EGFP
FM 4-64
Merge
Δmep1 Δmep3 Δnpr1
SD -N
Par32-EGFP
FM 4-64
Merge
Δmep1 Δmep3 Δnpr1

Fig. S4

A

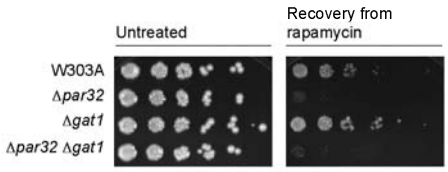
Untreated
Recovery from rapamycin
W303A
Δpar32
Δgat1
Δpar32 Δgat1

B

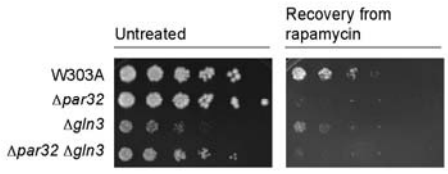
Untreated
Recovery from rapamycin
W303A
Δpar32
Δgln3
Δpar32 Δgln3

Fig. S5